



# Functionalisation of porous hydroxyapatite for bone substitutes

Edwige Meurice<sup>a,b</sup>, Anne Leriche<sup>a,b,\*</sup>, Jean-Christophe Hornez<sup>a,b</sup>, Franck Bouchart<sup>a,b</sup>,  
Emmanuelle Rguiti<sup>a,b</sup>, Laurent Boilet<sup>a,b</sup>, Michel Descamps<sup>a,b</sup>, Francis Cambier<sup>c</sup>

<sup>a</sup> Laboratoire des Matériaux Céramiques et Procédés Associés (LMCPA), Université Lille-Nord de France, F-59000 Lille, France

<sup>b</sup> UVHC, ZI Champ de l'Abbesse F-59600 Maubeuge, France

<sup>c</sup> Belgian Ceramic Research Centre (BCRC), Avenue Gouverneur Cornez, 4, B-7000 Mons, Belgium

## Abstract

Calcium phosphate ceramics such as hydroxyapatite (HA) have been widely used to repair and reconstruct damaged parts of the human skeleton. This material is currently available as injectable cements, granules or macroporous blocks. The most common materials are granules because of their ability to be implanted in the human body. In this study, a new manufacturing procedure to fabricate either dense or microporous or macroporous hydroxyapatite spherical granules based on a lost wax method and leading to beads with a fully controlled porosity was developed. The as-obtained HA granules porous structure was impregnated by gentamicin and lambda phage and the antibiotic and phage releasing kinetics were studied as a function of time and porosity.

© 2012 Elsevier Ltd. All rights reserved.

**Keywords:** B. Porosity; Hydroxyapatite; Beads; Functionalisation; Drug releasing; Phage therapy

## 1. Introduction

Bioceramic materials such as calcium phosphate ceramics, and in particular hydroxyapatite (HA) and  $\beta$  tricalcium phosphate ( $\beta$ -TCP) because of their excellent biocompatibility, bioactivity and osteoconduction properties, have been widely used to repair and reconstruct damaged parts of the human skeleton and especially as bone substitutes in the filling of bone defects.<sup>1</sup> These materials are available in the form of injectable cements, granules or macroporous blocks. Calcium phosphate granules have been generally selected for classical bone filling.<sup>2</sup> However, such granules present irregular shapes and do not allow for optimal filling of bone cavity or defect. To overcome this problem, adjunction of a binding agent such as fibrin glue has been found to stabilise the granules in the implantation site and produce a composite that can be moulded into the defect without empty spaces.<sup>3</sup>

Many processing routes have been used for fabrication of porous hydroxyapatite granules, such as hydrothermal conversion of natural corals,<sup>4</sup> crushing of sintered blocks, granulation

by vibration and rolling,<sup>5</sup> dripping procedure, casting in plaster mould, emulsion methods<sup>6</sup> and spray-drying. A new method similar to the lost wax process has been developed by our team. This method consists in building a calcium carbonate scaffold around a template constituted of piled up calibrated PMMA poly(methyl methacrylate) beads. Thermal treatment led to the removal of the organic beads, thus resulting in a porous calcium carbonate scaffold. This empty space could then be filled by a HA powder aqueous slurry and subsequent elimination of the carbonate scaffold allowed to obtain controlled size and shape HA beads.<sup>7</sup>

Besides their use as bone filling material, microporous HA beads could be used in the orthopaedic field as drug delivery carriers for substances such as growth factors, anticancer drugs and antibiotic agents. Microporous HA (i.e. with a pore size around the micrometer) could be obtained by partial sintering of the ceramic material. It was thus possible to impregnate them by active substances like gentamicin antibiotic for its prophylactic action<sup>8</sup> or phages used for phage therapy in case of nosocomial diseases.<sup>9</sup>

In this study, we present the fabrication process for dense, micro- and macro-porous HA beads from our lost wax process and we give comparative results of drug loading and release rate of gentamicin antibiotic and lambda phage in the microporous HA beads.

\* Corresponding author at: UVHC, ZI Champ de l'Abbesse F-59600 Maubeuge, France.

E-mail address: [anne.leriche@univ-valenciennes.fr](mailto:anne.leriche@univ-valenciennes.fr) (A. Leriche).

## 2. Experimental

### 2.1. HA powder synthesis

HA powder was prepared by an aqueous precipitation technique using a diammonium phosphate solution and a calcium nitrate solution. After successive steps of precipitation–calcination–milling, the as-obtained powder displayed a surface area of 5 m<sup>2</sup>/g, a mean particle size of 1 μm and a Ca/P ratio of 1.667.<sup>10</sup> A complete densification was achieved by pressureless sintering after 3 h at 1250 °C.

### 2.2. Fabrication of ceramic beads

The porous ceramic beads were fabricated through the lost wax process. The first step consisted in building a template of organic beads, infiltrating it by a calcium carbonate slurry and burning the organic species by thermal treatment. The as-resulting voids were then filled with a HA powder slurry and the carbonate surrounding carapace was destroyed by another thermal treatment (Fig. 1).

#### 2.2.1. Preparation of the organic skeleton

An organic skeleton was built by stacking PMMA beads (Diakon TM Ineos Acrylics Holland, Saluc Belgium) with diameters in the range from 100 μm to 3 mm. Bridging between polymeric beads was obtained by a chemical treatment under pressure using acetone (RPE 99.8% Carlo Erba, France) which

partially dissolved the PMMA bead surfaces and induced welding of the individual bodies (Fig. 1a).

#### 2.2.2. Preparation of the calcium carbonate scaffold

The as-prepared organic skeleton was then impregnated by the calcium carbonate suspension in order to fill the voids between polymeric PMMA beads.

A CaCO<sub>3</sub> powder (Mikhart 2, Provençale s.a, France) showing a surface area of 3.3 m<sup>2</sup>/g, a mean particle size of 3 μm and a purity level superior to 99% was used.

A 64 wt.% dry matter CaCO<sub>3</sub> aqueous slurry was prepared. Slurry deflocculating was assured by adding Darvan C (R.t.Vanderbilt. Co) in an amount corresponding to 1.5 wt.% of the CaCO<sub>3</sub> content. An organic binder (Duramax B1001, Rohm and Haas) in an amount equal to 4 wt.% of the CaCO<sub>3</sub> content was also added to ensure a consolidation of the green material during the thermal treatment necessary for PMMA elimination. Slip preparation was carried out using a planetary ball mill with agate container and balls. Milling duration was fixed to 1 h with a 180 rpm rotation speed. After the infiltration process (Fig. 1b), the sample was dried in a plaster mould and then underwent a two-dwell thermal treatment (220 °C during 20 h followed by 250 °C for 10 h). The elimination of PMMA beads created a controlled size macroporosity within the ceramic. After this thermal treatment, the 3% residual organic ensured enough mechanical strength for the handling of samples during the later stages and the sample was constituted of macropores, the size of which was equal to that of the used PMMA beads. These cavities were interconnected. Fig. 1b shows macroscopic and microscopic

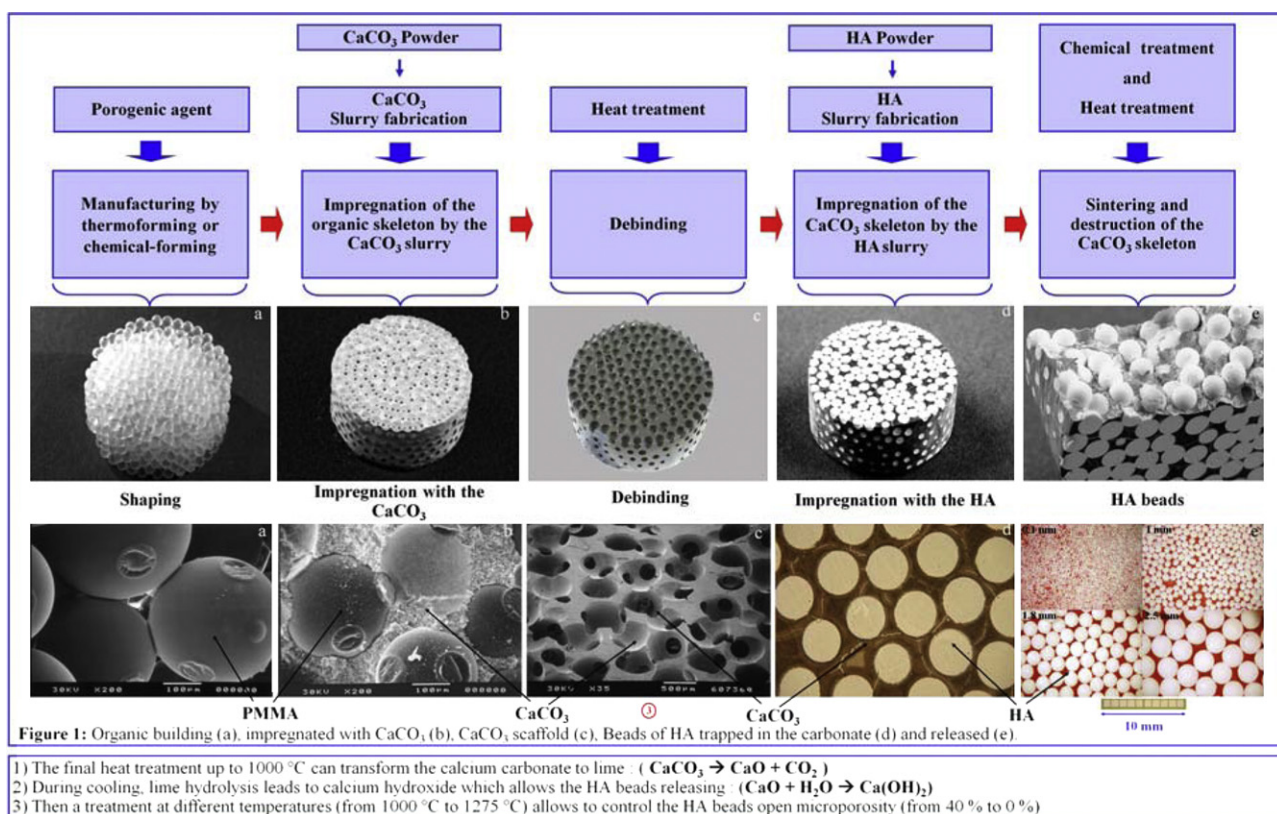


Fig. 1. HA spherical granules elaboration procedure.

views of a  $\text{CaCO}_3$  impregnated organic skeleton. The calcium carbonate scaffold after thermal treatment is presented in Fig. 1c.

### 2.2.3. Manufacturing of dense or microporous HA beads

HA aqueous slurries were prepared under the same experimental conditions as the  $\text{CaCO}_3$  suspensions with a 75 wt.% dry matter content, using 1.5 wt.% of Darvan C (relatively to the HA content).

The calcium carbonate scaffold was impregnated by aqueous suspensions of hydroxyapatite in order to fill the cavities left by the PMMA beads. This operation was performed into a plaster mould in order to enhance the drying.

Fig. 1d represents a macroscopic view of a polished  $\text{CaCO}_3$  scaffold filled with HA after drying. After filling of the  $\text{CaCO}_3$  scaffold by the HA powder, the material was heated up to  $1000^\circ\text{C}$  to change the calcium carbonate into lime and to induce a pre-sintering of the HA, which reinforced the ceramic beads in order to give them a better resistance during the subsequent destruction step of the calcium carbonate scaffold (see hereafter). A XRD analysis of a HA/ $\text{CaCO}_3$  powder mixture, heated up to  $1000^\circ\text{C}$ , did not show any chemical reaction between these two compounds.

During cooling, the samples were quenched into water from  $200^\circ\text{C}$ . Lime thereby transformed into calcium hydroxide, this reaction being accompanied by a significant swelling of the structure, which caused the  $\text{Ca}(\text{OH})_2$  new formed ceramic disintegration and the HA beads release. After this step, HA beads and  $\text{Ca}(\text{OH})_2$  powder were separated by mechanical sieving.

Fig. 1e shows a macroscopic view of HA beads obtained using a  $\text{CaCO}_3$  scaffold made from various PMMA calibrated beads with diameters in the range from  $100\text{ }\mu\text{m}$  to  $3\text{ mm}$ .

In order to obtain different porosity ranges, beads were sintered at different temperatures:  $1275$ ,  $1150$  and  $1100^\circ\text{C}$ . Sintering at the highest temperature allowed obtaining 97.5% as relative density and consequently the sample was free of open porosity and exhibited only 2.5% of closed porosity. On the contrary, the lowest temperatures ( $1150$  and  $1100^\circ\text{C}$ ) led to porous beads characterised by micronic open porosity volumes equal to 20% and 42%, respectively.

## 2.3. Application of microporous HA beads to the delivery of biological agents

### 2.3.1. Chemical functionalisation: antibiotic loading and release evaluation

At first, the microporous HA beads were impregnated with the broad-spectrum antibiotic gentamicin. HA beads with 20% of open porosity and diameters in the range from  $600$  to  $700\text{ }\mu\text{m}$  were vacuum impregnated with a solution of gentamicin (20 mg per gram of HA), and then dried at  $37^\circ\text{C}$  for 24 h. The impregnation efficiency was evaluated by thermogravimetric analysis. The drug release was measured by static and dynamic methods. For the static method, 1 g of the impregnated sample was plunged in different liquid media such as distilled water, a phosphate buffer solution (PBS) or simulated body fluid (SBF), in a  $50\text{ cm}^3$  cell, placed in an incubator at  $37^\circ\text{C}$  (Binder APT

line<sup>TM</sup> C150). Dynamic trials were also performed, using only distilled water as the media in order to show if there was a significant difference between the dynamic and static methods. For the dynamic method, 1 g of impregnated beads was placed in a  $2\text{ cm}^3$  flow cell thermostated by a digital dry bath (Fisher scientific FB15103). The fluid circulation was performed by a high precision tubing pump with planetary drive (ISMATEC IPC-N ISM936). Distilled water was used as solvent with a flow rate of  $6\text{ cm}^3/\text{min}$ .

Gentamicin release evaluation was performed at a 255 nm wave light on a UV-visible spectrophotometer (SHIMADZU UV-2500 PC). Using a calibration curve, the optical densities were converted to mg/ml of gentamicin. Data were recorded with a specific spectroscopy software (UV.Prob 2.21).

### 2.3.2. Biological functionalisation

#### 2.3.2.1. Bacterial strain, phage, media and growth conditions.

The bacterial strain used in this study were the  $\lambda$  phage-sensitive *Escherichia coli* K12 (A324). Bacteria were grown at  $37^\circ\text{C}$  under 170 rpm agitation in Luria-Bertani broth (LB - bactotrypton 5 g/l, yeast extract 10 g/l, NaCl 5 g/l, pH 7.2). For solid test, bacteria were grown on LB Agar (LB and agar 15 g/l) at  $37^\circ\text{C}$ . The  $\lambda$ vir phage was a modified lytic phage and stock solution was prepared by infection of A324.<sup>11</sup> HA samples were incubated 24 h in 5 ml of  $\lambda$ vir phage stock, and then rapidly washed once in LB medium to remove excess of phage suspension. Bacterial growth was measured by optical density at 620 nm ( $\text{OD}_{620}$ ). *E. coli* K12 (A324) was grown in 30 ml LB at  $37^\circ\text{C}$  under shaking with a starting  $\text{OD}_{620}$  of 0.03. At  $\text{OD}_{620}$  0.12, phage-loaded HA samples were added into the culture tubes. Growth was followed until complete lysis of bacteria or until stationary phase.

For solid test, the  $\lambda$  phage-loaded HA samples were washed in 30 ml LB medium at  $37^\circ\text{C}$  under 170 rpm shaking. LB medium was renewed after 3, 6, 18, 24 and 48 h. *E. coli* K12 was spread on LB agar plates in 3 ml R-Top medium (Bactotrypton 10 g/l, yeast extract 1 g/l, NaCl 8 g/l and agar 8 g/l) to promote  $\lambda$ vir phage diffusion. Then  $\lambda$  phage-loaded HA samples were placed on LB agar plates before R-Top medium solidification. Bacterial lysis was measured according to the standard disk-diffusion method.<sup>12</sup> After 48 h of incubation at  $37^\circ\text{C}$ , lysis plaques were measured and defined as the total diameter of the lysis plaque including the sample.

## 3. Results and discussion

### 3.1. Chemical functionalisation

Thermogravimetric analysis carried out on HA beads impregnated with gentamicin (Fig. 2) showed an initial weight loss of 0.4% between  $20$  and  $110^\circ\text{C}$  which corresponds to residual moisture. A second weight loss appeared from  $240^\circ\text{C}$ , and continued up to  $600^\circ\text{C}$ . This behaviour was induced by the gentamicin combustion, with a weight loss (2%) equal to the gentamicin weight introduced within HA beads. So, it shows that the whole gentamicin amount used for impregnation was completely



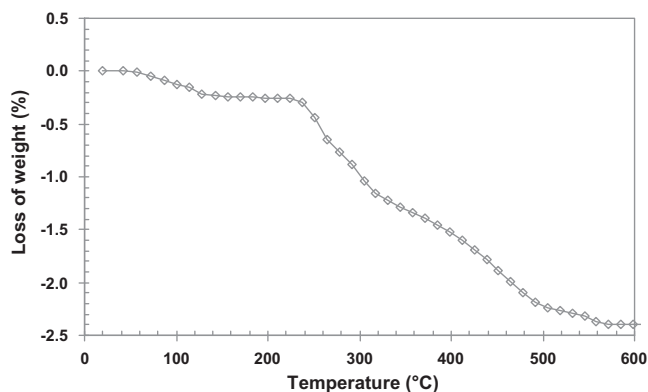


Fig. 2. Thermogravimetric analysis of gentamicin loaded HA 20 vol.% microporous beads (1150 °C).

soaked in the granules. In order to slacken the drug release, a partial polymer coating was applied on the impregnated beads as shown in Fig. 3a. To evaluate the drug release rate in close physiological environment conditions, the uncoated and coated gentamicin loaded granules were placed in a continuous distilled water flow (6 ml/h). Fig. 3 shows the released gentamicin amount versus time. Fig. 3a presents the dynamic release of gentamicin for beads characterised by an open porosity of 20 vol.% and a diameter in the range from 600 to 700  $\mu\text{m}$  without and with PMMA coating. In the case of coated loaded beads, only 75% of gentamicin was released whereas for uncoated beads

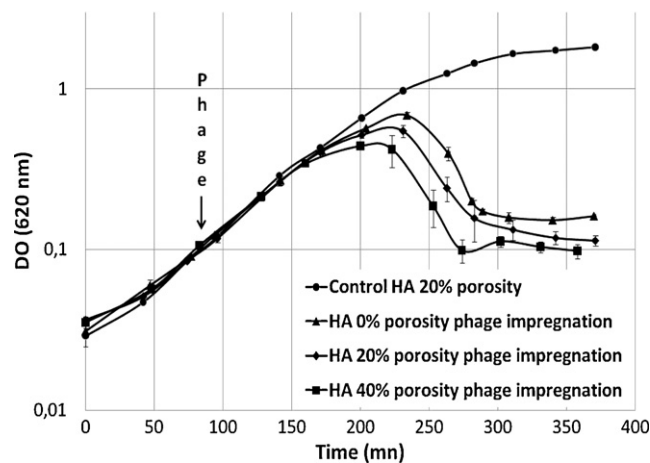


Fig. 4. Bacterial growth kinetics measured by optical density at 620 nm in presence of various porosity ceramic phage supports.

more than 90% of gentamicin was released after 24 h. After this time period, the released amount decreased during 5 days. The PMMA coating led to a decrease of the release kinetic of gentamicin and allowed the time of prophylactic effect to increase. Fig. 3b and c respectively present the results of static release of gentamicin for beads presenting various porosity levels (from 0 to 30 vol.%) and for beads with 30 vol.% porosity in different liquid media such as water, PBS and SBF, with an adjusted pH of 7.4 for all solutions. As expected, the amount of impregnated

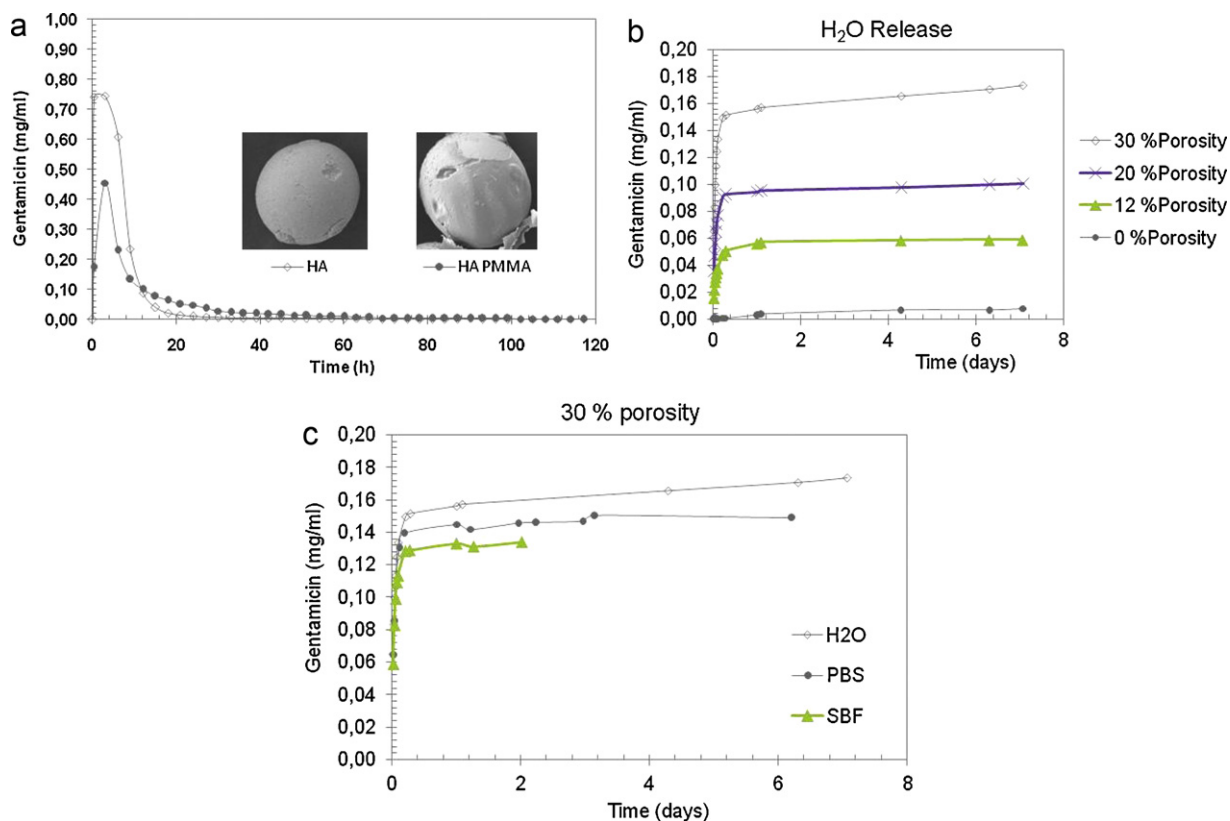


Fig. 3. (a) Dynamic release of gentamicin measured by UV-visible spectrophotometry at 255 nm from loaded HA and PMMA coated microporous beads (20 vol.%). (b) Static release of gentamicin measured by UV-visible spectrophotometry at 255 nm from loaded bioceramic microporous sample with different porosity. (c) Static release of gentamicin measured by UV-visible spectrophotometry at 255 nm from loaded bioceramic 30% microporous sample in various liquid media.

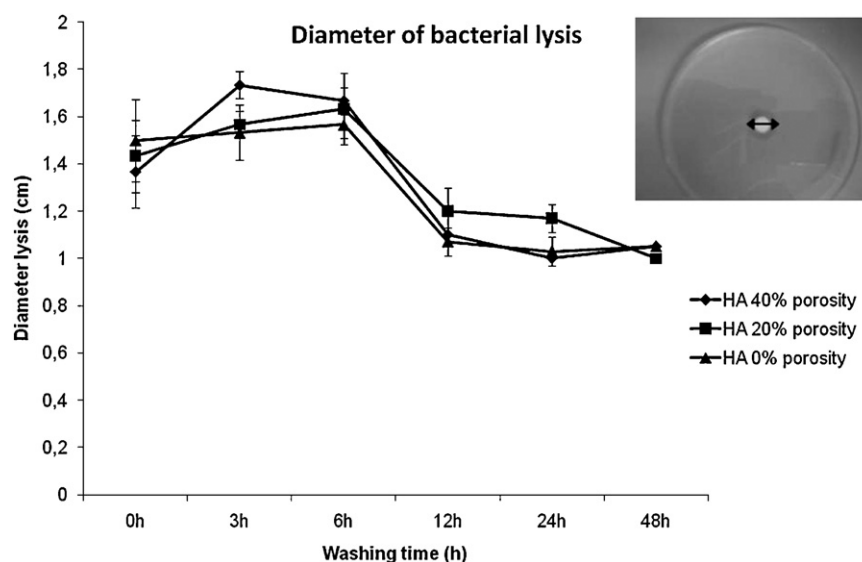


Fig. 5. Diameter of bacterial lysis plaques in presence of various porosity ceramic phage supports according to the washing time in LB medium. Picture shows an example of lysis plaque diameter.

gentamicin increased with the beads porosity. It can also be noted that the liquid nature influenced the release kinetic depending on the solution ionic strength.

### 3.2. Biological functionalisation

Fig. 4 shows the bacterial lysis efficiency of  $\lambda$  phage-loaded HA samples according to their microporous volume. The different microporous volumes were obtained by sintering HA samples at different temperatures. Control HA was a sample without  $\lambda$ -phage impregnation. The  $\lambda$  phage-loaded HA samples were added after two generation times of bacteria and bacterial lysis occurred about 90 min later. The lysis started earlier and was faster for samples with the largest microporous volumes as shown by the fact that HA with 40% of porosity (sintered at 1100 °C) had a faster kinetic than dense samples (sintered at 1275 °C). It is interesting to note that dense HA samples also had an antibacterial effect suggesting that the  $\lambda$  bacteriophage strongly interacted with the HA ceramic surface.

Fig. 5 shows the time release ability of  $\lambda$  phage-loaded HA samples according to their microporosity. The phage-loaded HA samples were washed in LB medium to check the time retention as a function of the HA sample porosities. *E. coli* K12 was homogeneously spread on LB agar plates and the different washed phage-loaded HA samples were introduced. Diameter of lysis plaques was measured 48 h later. Release of phages from all the HA samples was nearly constant in the first 6 h of washing. After 18 h and until 48 h of washing, diameter of lysis plaques decreased by 30% for each sample. These results suggest that HA samples are able to retain phages and to release them several days later, even for dense materials.

## 4. Conclusions

These first experiments revealed that microporous HA microspheres can be used as a matrix for local drug delivery to prevent and curate infections associated to bone implants. The drug release quantity and duration could be controlled by the morphology and microstructure of HA beads and in particular by the porosity, which is encouraging for the development of a drug delivery system meeting the therapeutic dosage criteria.

## Acknowledgements

The present research work has been supported by the Nord-Pas-de-Calais Region, the European Regional Development Fund (ERDF) through Interreg IVA France-Wallonie-Vlaanderen Programme, the Regional Delegation for Research and Technology, the Ministry of Higher Education and Research. The authors gratefully acknowledge the support of these institutions.

## References

1. Burg KJL, Porter S, Kellam JF. Biomaterial developments for bone tissue engineering. *Biomaterials* 2000;**21**:2347–59.
2. Daculsi G, LeGeros RZ, Heughebaert M, Barbieux I. Formation of carbonate-apatite crystals after implantation of calcium phosphate ceramics. *Calcif Tissue Int* 1990;**46**:20–7.
3. Le Nihouannen D, Le Guehennec L, Rouillon T, Pilet P, Melitta Bilban M, Layrolle P, Daculsi G. Micro-architecture of calcium phosphate granules and fibrin glue composites for bone tissue engineering. *Biomaterials* 2006;**27**:2716–22.
4. Roy DM, Linnehan SK. Hydroxyapatite formed from coral skeletal carbonate by hydrothermal exchange. *Nature* 1974;**247**:220–2.
5. Zhang X, Chen J, Zhou J. Porous hydroxyapatite granules: their synthesis applications and characterization. *Clin Mater* 1989;**4**:319–27.

6. Lee JS, Park JK. Processing of porous ceramic spheres by pseudo-double-emulsion method. *Ceram Int* 2003;**29**:271–8.
7. Descamps M, Hornez JC, Leriche A. Manufacture of hydroxyapatite beads for medical applications. *J Eur Ceram Soc* 2009;**29**(3):369–75.
8. Sivakumar M, Panduranga Rao K. Preparation, characterization and in vitro release of gentamicin from coralline hydroxyapatite gelatin composite microspheres. *Biomaterials* 2002;**23**(August (15)):3175–81.
9. John NH, Nicholas HM. Phage therapy. *Drug Discov Today* 2009;**14**(June (11–12)):536–40.
10. Hornez JC, Chai F, Monchau F, Blanchemain N, Descamps M, Hildebrand HF. Biological and physico-chemical assessment of hydroxyapatite (HA) with different porosity. *Biomol Eng* 2007;**24**:505–9.
11. Jacob F, Wollman EL. Induction spontanée du développement du bacteriophage  $\lambda$  au cours de la recombinaison génétique, chez *E. coli* K-12. *Compt Rend Acad Sci Paris* 1954;**239**:317–9.
12. Biedenbach DJ, Jones RN. Disk diffusion test interpretive criteria and quality control recommendations for testing linezolid (U-100776) and eperezolid (U-100592) with commercially prepared reagents. *J Clin Microbiol* 1997;**35**:3198–202.